

CERN-PH-EP-2012-229
08 August 2012

Measurement of electrons from beauty hadron decays in pp collisions at $\sqrt{s} = 7$ TeV

ALICE Collaboration*

Abstract

The production cross section of electrons from semileptonic decays of beauty hadrons was measured at mid-rapidity ($|y| < 0.8$) in the transverse momentum range $1 < p_T < 8$ GeV/ c with the ALICE experiment at the CERN LHC in pp collisions at a center of mass energy $\sqrt{s} = 7$ TeV using an integrated luminosity of 2.2 nb^{-1} . Electrons from beauty hadron decays were selected based on the displacement of the decay vertex from the collision vertex. A perturbative QCD calculation agrees with the measurement within uncertainties. The data were extrapolated to the full phase space to determine the total cross section for the production of beauty quark-antiquark pairs.

arXiv:1208.1902v4 [hep-ex] 20 Jun 2016

*See Appendix A for the list of collaboration members

The measurement of heavy-flavor (charm and beauty) production in proton–proton (pp) collisions at the CERN Large Hadron Collider (LHC) provides a crucial testing ground for quantum chromodynamics (QCD), the theory of strong interactions, in a new high-energy regime. Because of their large masses heavy quarks are mainly produced via initial hard parton-parton collisions, even at low transverse momenta p_T . Therefore, heavy-flavor production cross sections constitute a prime benchmark for perturbative QCD (pQCD) calculations. Furthermore, heavy-flavor measurements in pp collisions provide a mandatory baseline for corresponding studies in nucleus-nucleus collisions. Heavy quark observables are sensitive to the properties of the strongly interacting partonic medium which is produced in such collisions.

Earlier measurements of beauty production in $p\bar{p}$ collisions at $\sqrt{s} = 1.96$ TeV at the Tevatron [1] are in good agreement with pQCD calculations at fixed order with next-to-leading log resummation (FONLL) [2, 3]. Measurements of charm production, available at high p_T only [4], are close to the upper limit but still consistent with such pQCD calculations. The same trend was observed in pp collisions at $\sqrt{s} = 0.2$ TeV at RHIC [5, 6].

In pp collisions at the LHC, heavy-flavor production was investigated extensively at $\sqrt{s} = 7$ TeV in various decay channels. With LHCb beauty hadron production cross sections were measured at forward rapidity [7] and, at high p_T only, with CMS at mid-rapidity [8]. At low p_T , mid-rapidity J/ψ meson production from beauty hadron decays was studied with ALICE [9]. These results, as well as the mid-rapidity D-meson production cross sections measured with ALICE [10], are well described by FONLL pQCD calculations. The same is true for the production cross sections of electrons and muons from semileptonic decays of heavy-flavor hadrons reported by ATLAS [11] at high p_T , and by ALICE down to low p_T [12, 13]. However, still missing at the LHC is the separation of leptons from charm and beauty hadron decays at low p_T , which is important for the total beauty production cross section and which provides a crucial baseline for Pb-Pb collisions.

This Letter reports the mid-rapidity ($|y| < 0.8$) production cross section of electrons, $(e^+ + e^-)/2$, from semileptonic beauty hadron decays measured with the ALICE experiment in the range $1 < p_T < 8$ GeV/c in pp collisions at $\sqrt{s} = 7$ TeV. Two independent techniques were used for the separation of beauty hadron decay electrons from those originating from other sources, in particular charm hadron decays. The resulting invariant cross sections of electrons from beauty and from charm hadron decays are compared with corresponding predictions from a FONLL pQCD calculation. In addition, the measured cross sections were extrapolated to the full phase space and the total beauty and charm production cross sections were determined.

The data set used for this analysis was recorded during the 2010 LHC run with ALICE, which is described in detail in [14]. Charged particle tracks were reconstructed in the pseudorapidity range $|\eta| < 0.8$ with the Time Projection Chamber (TPC) and the Inner Tracking System (ITS) which, in addition, provides excellent track spatial resolution at the interaction point. Electron candidates were selected with the TPC and the Time-Of-Flight detector (TOF). Data were collected using a minimum bias (MB) trigger [12] derived from the VZERO scintillator arrays and the Silicon Pixel Detector (SPD), which is the innermost part of the ITS consisting of two cylindrical layers of hybrid silicon pixel assemblies. The MB trigger cross section $\sigma_{\text{MB}} = 62.2 \pm 2.2$ mb [15] was measured in a van-der-Meer scan. An integrated luminosity of 2.2 nb^{-1} was used for this analysis.

Pile-up events were identified by requiring no more than one primary vertex to be reconstructed with the SPD as discussed in [12]. Taking into account the efficiency of the pile-up event identification, only 2.5% of the triggered events suffered from pile-up. The corresponding events were removed from the analyzed data sample. The systematic uncertainty due to the remaining undetected pile-up events was negligible.

Events and tracks were selected following the approach from a previous analysis [12]. Charged particle

tracks reconstructed in the TPC and ITS were propagated towards the outer detectors using a Kalman filter approach [16]. Geometrical matching was applied to associate tracks with hits in the outer detectors. To guarantee good particle identification based on the specific dE/dx in the TPC, tracks were required to include a minimum number of 80 clusters used for the energy loss calculation. A cut on the number of clusters for tracking is used to enhance the electron/pion separation. The stringent request for at least 120 clusters from the maximum of 159 enhances electrons relative to hadrons. In total, at least four ITS hits were required to be associated with a track. A cut on the distance of closest approach (DCA) to the primary vertex in the plane perpendicular to the beam axis (xy) as well as in the beam direction (z) was applied to reject background tracks and non-primary tracks. Differently from the heavy-flavor electron analysis [12], the pseudorapidity range was extended to $|\eta| < 0.8$, and tracks were required to be associated with hits in both layers of the SPD in order to minimize the contribution from tracks with randomly associated hits in the first pixel layer. The latter criterion provides a better measurement of the track's transverse impact parameter d_0 , i.e. the DCA to the primary collision vertex in the plane perpendicular to the beam axis, where the sign of d_0 is attributed on the basis of the relative position of primary vertex and the track prolongation in the direction perpendicular to the direction of the transverse momentum vector of the track.

Electron candidates were required to be consistent within three standard deviations with the electron time of flight hypothesis, thus efficiently rejecting charged kaon background up to momenta of ≈ 1.5 GeV/ c and proton background up to ≈ 3 GeV/ c . Additional background, in particular from charged pions, was rejected using the specific energy loss, dE/dx , measured for charged particles in the TPC.

Due to their long lifetime ($c\tau \sim 500$ μm), beauty hadrons decay at a secondary vertex displaced in space from the primary collision vertex. Consequently, electron tracks from semileptonic beauty hadron decays feature a rather broad d_0 distribution, as indicated by simulation studies in Fig. 1(a). Also shown are the d_0 distributions of the main background sources, i.e. electrons from charm hadron decays, from Dalitz and dilepton decays of light mesons, and from photon conversions. These distributions were obtained from a detailed Monte Carlo simulation of the experiment using GEANT3 [17]. With the PYTHIA 6.4.21 event generator [18] pp collisions were produced employing the Perugia-0 parameter tuning [19]. The p_T shapes of beauty hadron decay electrons from a FONLL pQCD calculation [20] and from PYTHIA are in good agreement. The PYTHIA simulation does not reproduce precisely the p_T -differential yields of background sources measured in data. Therefore, the p_T distributions of the relevant electron sources in PYTHIA were re-weighted to match the distributions measured with ALICE, prior of propagation through the ALICE apparatus using GEANT3. After the full Monte Carlo simulation, the same event cuts and track selection criteria (including that on d_0) as in data were applied. The p_T distributions of the backgrounds were normalized by the number of events passing these event selection cuts, corrected for the efficiency to reconstruct a primary vertex. Background electrons surviving these selection criteria were subtracted from the inclusive electron spectrum obtained from data. This approach relies on the availability of the p_T -differential cross section measurements of the main background sources.

The production cross sections of π^0 and η mesons, the dominant sources of electrons from Dalitz decays and from photons which convert in material into e^+e^- pairs, were measured with ALICE in pp collisions at $\sqrt{s} = 7$ TeV [21]. The conversion electron yield depends on the material budget which was measured with a systematic uncertainty of 4.5% [21]. Other light hadrons and heavy quarkonia contribute through their decays to the electron spectrum and their phase space distributions were calculated with the approach described in [12]. This calculation also includes real and virtual photon production via partonic hard scattering processes. D^0 , D^+ , and D_s^+ meson production cross sections were measured with ALICE [10, 22] in the transverse momentum ranges $1 < p_T < 16$ GeV/ c , $1 < p_T < 24$ GeV/ c , and $2 < p_T < 12$ GeV/ c , respectively. Based on a FONLL pQCD calculation [20] the measured p_T -differential cross sections were extrapolated to $p_T = 50$ GeV/ c . The contribution from the unmeasured high- p_T region to the electron yield from D-meson decays was estimated to be $\leq 10\%$ for electrons

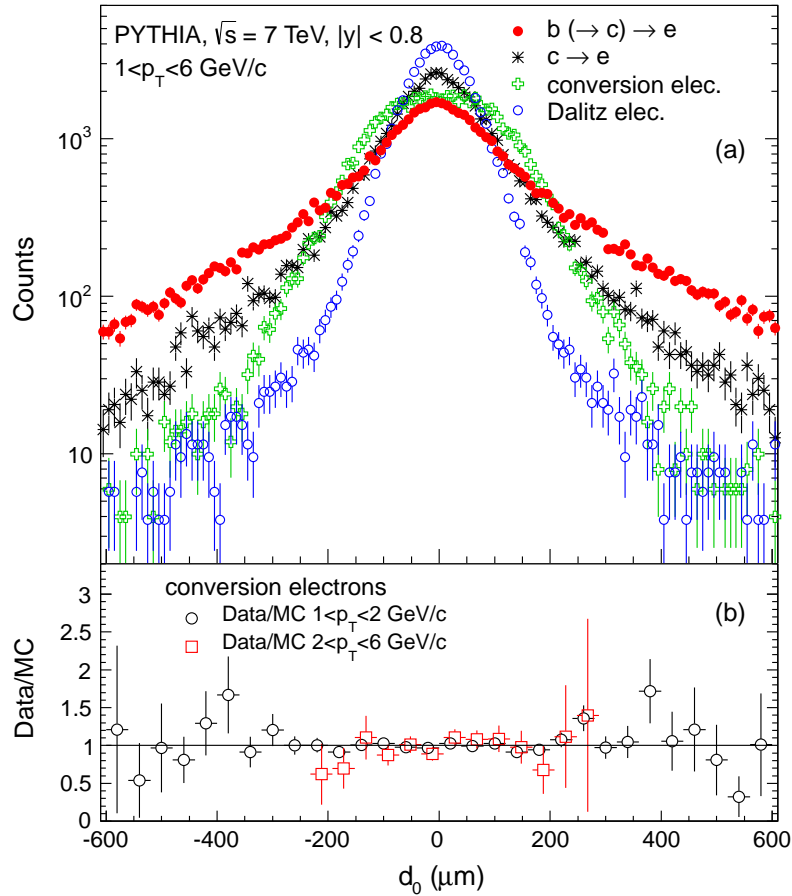


Fig. 1: (Color online) (a) d_0 distributions of electrons from beauty and charm hadron decays as well as from decays of light hadrons and from photon conversions obtained from PYTHIA simulations in the electron p_T range $1 < p_T < 6$ GeV/c. The distributions were normalized to the same integrated yield. (b) Ratios of the measured and the simulated d_0 distributions of conversion electrons in the ranges $1 < p_T < 2$ GeV/c and $2 < p_T < 6$ GeV/c (points shifted in d_0 by $10 \mu\text{m}$ for better visibility).

with $p_T < 8$ GeV/c. A contribution from Λ_c decays was included using a measurement of the ratio $\sigma(\Lambda_c)/\sigma(D^0 + D^+)$ from ZEUS [23].

The measured p_T spectra of the main background sources drop more quickly with p_T than the ones generated by PYTHIA for $p_T > 1$ GeV/c. The ratio of the measured yield and the yield from PYTHIA, which was used to weight the spectra of the electron sources in PYTHIA, is 1.3 (0.6) at $p_T = 1$ (10) GeV/c for π^0 . The corresponding ratio is 2.4 (1.3) at $p_T = 1$ (10) GeV/c for η mesons, and 0.95 (0.2) at $p_T = 1$ (10) GeV/c for electrons from charm hadron decays.

A cut on the d_0 parameter is applied in order to enhance the signal-to-background ratio (S/B) of electrons from beauty hadron decays. For this, it is crucial that the d_0 resolution is properly reproduced in the simulation. The d_0 resolution is found to be $80 \mu\text{m}$ ($30 \mu\text{m}$) for tracks with $p_T = 1$ (10) GeV/c [10]. The agreement of the d_0 measurement of electron candidates with the simulation is demonstrated in Fig. 1(b), which shows the ratios of the measured d_0 distribution to the one from simulation in the p_T ranges $1 < p_T < 2$ GeV/c and $2 < p_T < 6$ GeV/c for electrons from photon conversions, which is the only identifiable source in data. A pure sample of electrons from photon conversions in the detector material was identified using a V0-finder and topological cuts [24]. At $p_T > 6$ GeV/c, the number of reconstructed conversions was statistically insufficient for this cross check. In addition, the d_0 resolution

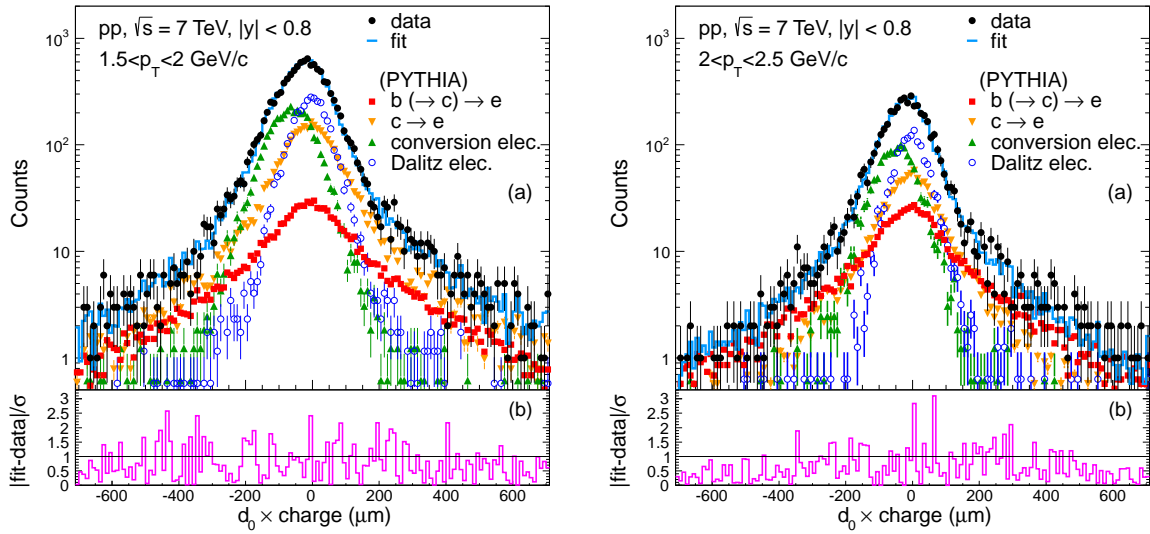


Fig. 2: (Color online) (a) Distribution of $d_0 \times \text{charge}$ for electron candidates after all analysis cuts (except that on d_0) superimposed to the best-fit result. The fit function is defined as the sum of the Monte Carlo d_0 distribution of beauty electrons and those of electrons from all other sources, the normalizations being the free parameters in the fit. The error bars represent the statistical uncertainties. (b) Differences between the data and the best fit result divided by the statistical error.

measured for charged tracks in data is reproduced within 10 % by the Monte Carlo simulation [10]. The difference in the particle multiplicities between data and simulation gives an effect on the primary vertex resolution, which is included in the d_0 resolution as a convolution of the track position and the primary vertex resolution. The Monte Carlo simulation shows that the electron Bremsstrahlung effect is limited to transverse momenta below 1 GeV/c. At higher p_T , the particle species dependences of the d_0 resolution is negligible.

Figure 2 shows that the d_0 distribution of the data sample is well described by the cocktail of signal and background. The measured d_0 distribution of identified electrons was fitted by minimizing a χ^2 between the measured d_0 distribution and the sum of the Monte Carlo d_0 distributions of signal and background in the corresponding electron p_T range. The differences between the data and the cocktail are consistent with statistical variations. The ratio of the signal to background yields, which is obtained by this fit procedure, agrees with that obtained in the present analysis within statistical uncertainties.

The widths of the d_0 distributions depend on p_T . Only electrons satisfying the condition $|d_0| > 64 + 780 \times \exp(-0.56 p_T)$ (with d_0 in μm and p_T in GeV/c) were considered for the further analysis. This p_T -dependent d_0 cut was determined from the simulation to maximize the significance for the beauty decay electron spectrum. The possible bias introduced by this optimization is taken into account in the estimation of the systematic uncertainties, by varying substantially the cut value.

Fits of the TPC dE/dx distribution in momentum slices indicate that the remaining hadron contamination grows from less than 10^{-5} at 1 GeV/c to $\approx 20\%$ at 8 GeV/c before the application of the d_0 cut. Since hadrons originate from the primary collision vertex, the latter cut reduces the remaining hadron contamination to less than 3% even at the highest p_T considered here. The electron background from sources other than beauty hadron decays was estimated based on the method described above. In Figure 3 the raw electron yield, as well as the non-beauty electron background yield, which is subtracted in the analysis, are shown after the application of the track selection criteria. At $p_T = 1$ GeV/c, the background contributions from charm hadron decays, light meson decays, and photon conversions are approximately equal and S/B is $\approx 1/3$. At $p_T = 8$ GeV/c, the background originates mostly from charm hadron decays

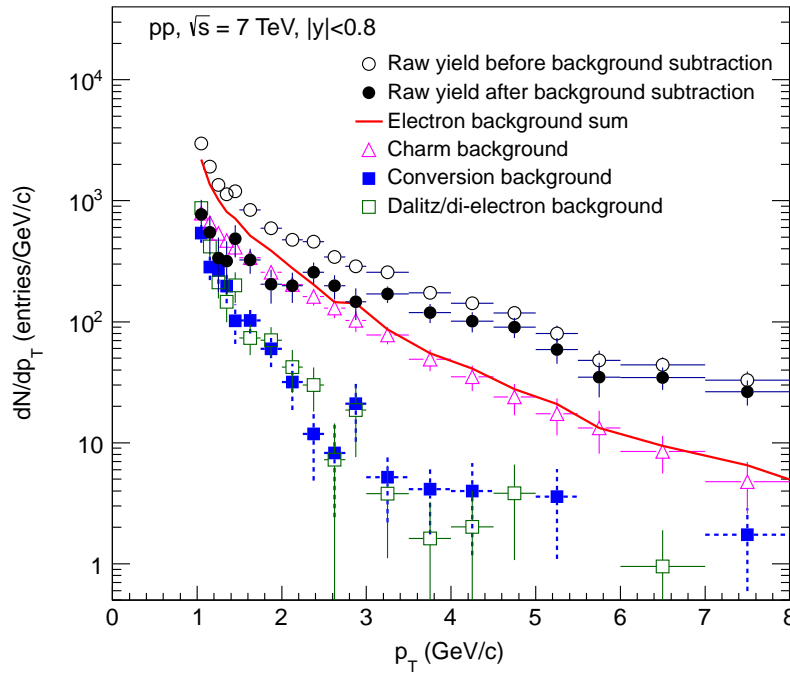


Fig. 3: (Color online) The signal (black solid circle) and the background yields after the application of the track selection criteria including the one on d_0 . The background electrons (red solid line), i.e. the sum of the electrons from charm hadron decays, from Dalitz and dilepton decays of light mesons, and from photon conversions, were subtracted from the inclusive electron spectrum (black open circle). The error bars represent the statistical uncertainties. The symbols are plotted at the center of each bin.

and S/B is ≈ 5 .

The electron yield from beauty hadron decays, $N_e(p_T)$, was corrected for the geometrical acceptance, the track reconstruction efficiency, the electron identification efficiency, and the efficiency of the d_0 cut. The total efficiency ε is the product of these individual factors. ε was computed from a full detector simulation using GEANT3 as discussed in [12]. In addition, the electron p_T distribution was corrected for effects of finite momentum resolution and energy loss due to Bremsstrahlung via a p_T unfolding procedure which does not depend on the p_T shape of Monte Carlo simulation [12].

The invariant cross section of electron production from beauty hadron decays in the range $|y| < 0.8$ was then calculated using the corrected electron p_T spectrum, the number of minimum bias pp collisions N_{MB} , and the minimum bias cross section σ_{MB} as

$$\frac{1}{2\pi p_T} \frac{d^2\sigma}{dp_T dy} = \frac{1}{2\pi p_T^\xi} \frac{N_e(p_T)}{\Delta y \Delta p_T} \frac{1}{\varepsilon} \frac{\sigma_{MB}}{N_{MB}}, \quad (1)$$

where p_T^ξ are the centers of the p_T bins with widths Δp_T and $\Delta y = 0.8$ is the width of the rapidity interval.

A summary of the estimated relative systematic uncertainties is provided in Table 1. The systematic uncertainties for the tracking and the particle identification are the following: the corrections of the ITS, TPC, TOF tracking efficiencies, the TOF, TPC particle identification efficiencies, the p_T unfolding procedure. These amount to $^{+17}_{-14}({}^{+8}_{-14})\%$ for $p_T < (>) 3$ GeV/c. Additional systematic uncertainties specific for this analysis due to the d_0 cut, the subtraction of the light hadron decay background and charm hadron decay background were added in quadrature. The systematic uncertainty induced by the d_0 cut was evaluated by repeating the full analysis with modified cuts. The variation of this cut was chosen such that it corresponds to $\pm 1\sigma$, where σ is the d_0 resolution measured on data [10]. These vary

Table 1: Overview of the contributions to the systematic uncertainties. The total systematic uncertainty is calculated as the quadratic sum of all contributions.

p_T range (GeV/c)	1 – 8
Error source	systematic uncertainty [%]
Track matching	± 2
ITS number of hits	$+1$ -4
TPC number of tracking clusters	$+15$ ($+3$) for $p_T < 2.5$ (> 2.5) GeV/c -7 (-4)
TPC number of PID clusters	± 2
DCA to primary vertex in xy (z)	± 1
TOF matching and PID	± 5
TPC PID	$+5$ ($+2$) for $p_T < 3$ (> 3) GeV/c -5
Minimum d_0 cut	± 12
Charge dependence	$+1$ -7
η dependence	-6
Unfolding	± 5
Light hadron decay background	≈ 10 (< 2) for $p_T = 1$ (> 2) GeV/c
Charm hadron decay background	≈ 30 (< 10) for $p_T = 1$ (> 3) GeV/c

the minimum d_0 cut efficiency by $\pm 20\%$. In addition, the full analysis was repeated after smearing the d_0 resolution in the Monte Carlo simulation by 10% [10], considering the maximum differences in the d_0 distribution in data and simulation. The uncertainty due to the background subtraction was evaluated by propagating the statistical and systematic uncertainties of the light and charm hadron measurements used as analysis input. At low p_T , the uncertainties are dominated by the subtraction of charm hadron decay background.

Figure 4 presents the invariant production cross section of electrons from beauty hadron decays obtained with the analysis based on the d_0 cut. As a cross check the corresponding result from an alternative method is shown. In the latter, the decay electron spectrum was calculated for charm hadrons as measured with ALICE [10] based on a fast Monte Carlo simulation using PYTHIA decay kinematics, and it was subtracted from the electron spectrum measured for all heavy-flavor hadron decays [12]. The systematic uncertainties of these two inputs have been added in quadrature as they are uncorrelated. The results from the subtraction method, which does not use a d_0 cut, and from the analysis based on the d_0 selection agree within the experimental uncertainties, which are much smaller, in particular at low p_T , for the beauty measurement employing the d_0 cut.

In Fig. 5(a) FONLL pQCD predictions [20] of the electron production cross sections are compared with the measured electron spectrum from beauty hadron decays and with the calculated electron spectrum from charm hadron decays. The ratios of the measured cross sections to the FONLL predictions are shown in Fig. 5(b) and 5(c) for electrons from beauty and charm hadron decays, respectively. The FONLL predictions are in good agreement with the data. At low p_T , electrons from heavy-flavor hadron decays originate predominantly from charm hadrons. As demonstrated in Fig. 5(d), beauty hadron decays take over from charm as the dominant source of electrons from heavy-flavor hadron decays close to electron transverse momenta of 4 GeV/c.

The integrated cross section of electrons from beauty hadron decays was measured as $6.61 \pm 0.54(\text{stat})_{-1.86}^{+1.92}(\text{sys}) \mu\text{b}$ for $1 < p_T < 8$ GeV/c in the range $|y| < 0.8$. The beauty production cross section $\sigma_{b\bar{b}}$ was calculated by extrapolating this p_T -integrated visible cross section down to $p_T = 0$ and to the full y range. The extrapolation factor was determined based on FONLL as described in [9], using the beauty to electron branching ratio $\text{BR}_{H_b \rightarrow e} + \text{BR}_{H_b \rightarrow H_c \rightarrow e} = 0.205 \pm 0.007$ [25]. The related uncertainty was obtained as the quadratic sum of the uncertainties from the beauty quark mass, from perturbative scales, and from

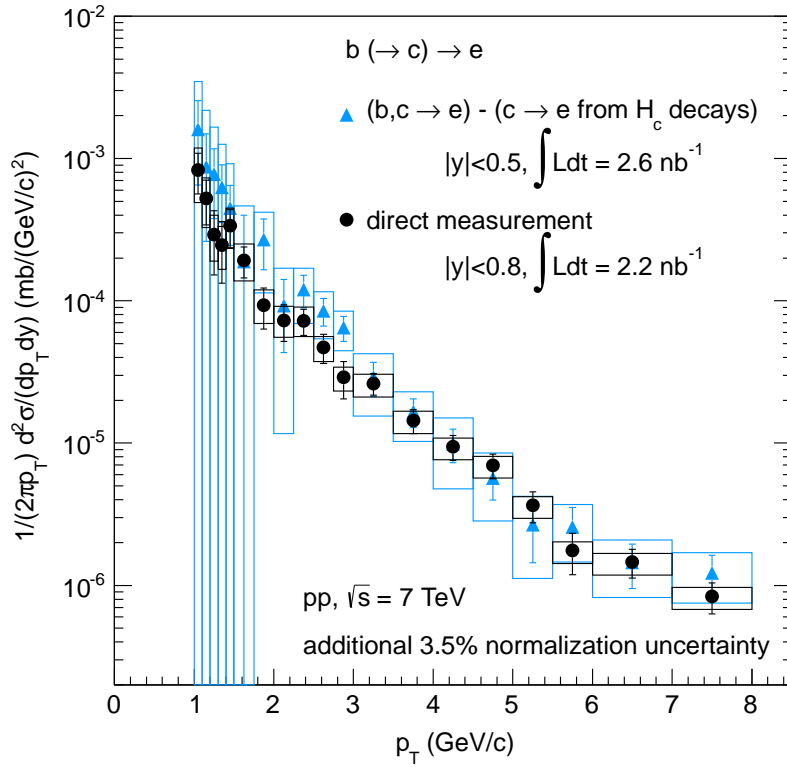


Fig. 4: (Color online) Invariant cross sections of electrons from beauty hadron decays measured directly via the transverse impact parameter method and indirectly via subtracting the calculated charm hadron decay contribution from the measured heavy-flavor hadron decay electron spectrum [12]. The error bars (boxes) represent the statistical (systematic) uncertainties.

the CTEQ6.6 parton distribution functions [26]. At mid-rapidity the beauty production cross section per unit rapidity is $d\sigma_{b\bar{b}}/dy = 42.3 \pm 3.5(\text{stat})^{+12.3}_{-11.9}(\text{sys})^{+1.1}_{-1.7}(\text{extr}) \mu\text{b}$, where the additional systematic uncertainty due to the extrapolation procedure is quoted separately. The total cross section was derived as $\sigma_{b\bar{b}} = 280 \pm 23(\text{stat})^{+81}_{-79}(\text{sys})^{+7}_{-8}(\text{extr}) \pm 10(\text{BR}) \mu\text{b}$, consistent with the result of a previous measurement of J/ψ mesons from beauty hadron decays $\sigma_{b\bar{b}} = 282 \pm 74(\text{stat})^{+58}_{-68}(\text{sys})^{+8}_{-7}(\text{extr}) \mu\text{b}$ [9]. The weighted average of the two measurements was calculated based on the procedure described in [27]. The statistical and systematic uncertainties of two measurements are largely uncorrelated, but the extrapolation uncertainties using the same theoretical model (FONLL) are correlated. The weights, defined using the statistical and the uncorrelated systematic uncertainties, and the correlated extrapolation uncertainties, are calculated as 0.499 for the measurement using semileptonic beauty hadron decays and 0.501 for that using non-prompt J/ψ mesons. The combined total cross section is $\sigma_{b\bar{b}} = 281 \pm 34(\text{stat})^{+53}_{-54}(\text{sys})^{+7}_{-8}(\text{extr}) \mu\text{b}$. FONLL predicts $\sigma_{b\bar{b}} = 259^{+120}_{-96} \mu\text{b}$ [20].

The production cross section of electrons from heavy-flavor hadron decays was measured as $37.7 \pm 3.2(\text{stat})^{+13.3}_{-14.4}(\text{sys}) \mu\text{b}$ for $0.5 < p_T < 8$ GeV/c in the range $|y| < 0.5$ [12]. After subtraction of the contribution from beauty hadron decays (see above) the resulting production cross section of electrons from charm hadron decays was converted into a charm production cross section applying the same extrapolation method as for beauty. With the branching ratio $\text{BR}_{H_c \rightarrow e} = 0.096 \pm 0.004$ [25], at mid-rapidity the charm production cross section per unit rapidity is $d\sigma_{c\bar{c}}/dy = 1.2 \pm 0.2(\text{stat}) \pm 0.6(\text{sys})^{+0.2}_{-0.1}(\text{extr})$ mb. The total cross section $\sigma_{c\bar{c}} = 10.0 \pm 1.7(\text{stat})^{+5.1}_{-5.5}(\text{sys})^{+3.5}_{-0.5}(\text{extr}) \pm 0.4(\text{BR})$ mb is consistent with the result of a previous, more accurate measurement using D mesons $\sigma_{c\bar{c}} = 8.5 \pm 0.5(\text{stat})^{+1.0}_{-2.4}(\text{sys})^{+5.0}_{-0.4}(\text{extr})$ mb [28]. The FONLL prediction is $\sigma_{c\bar{c}} = 4.76^{+6.44}_{-3.25}$ mb [20]. All measured

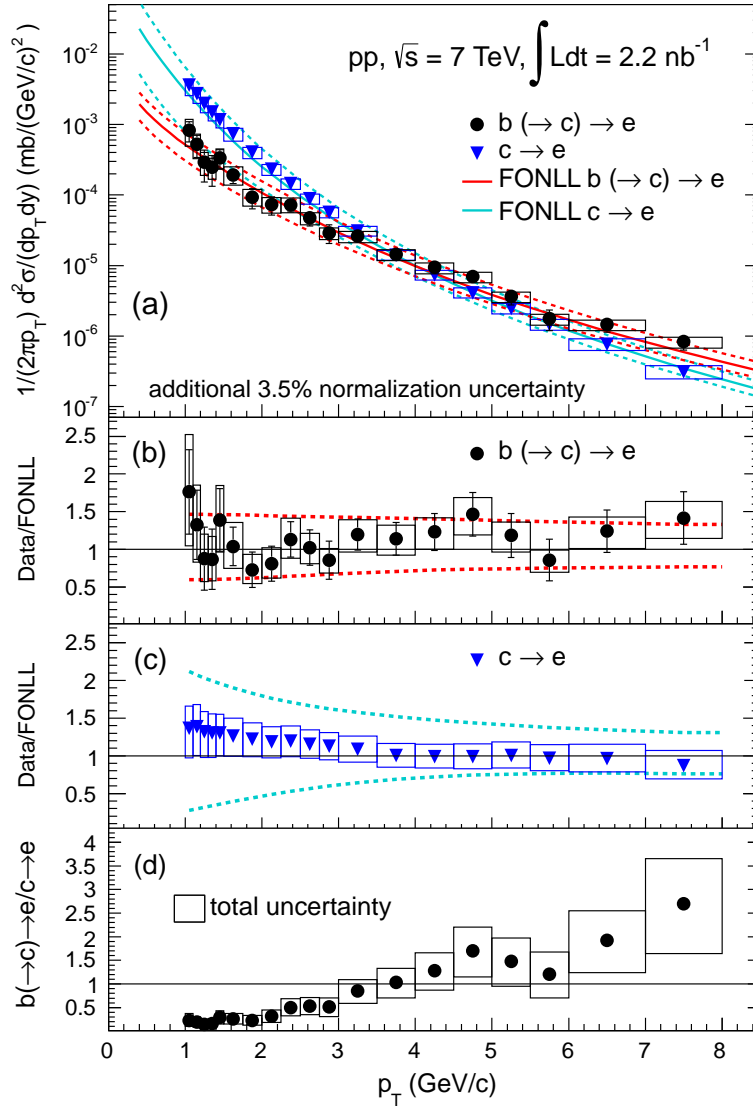


Fig. 5: (Color online) (a) p_T -differential invariant cross sections of electrons from beauty and from charm hadron decays. The error bars (boxes) represent the statistical (systematic) uncertainties. The solid (dashed) lines indicate the corresponding FONLL predictions (uncertainties) [20]. Ratios of the data and the FONLL calculations are shown in (b) and (c) for electrons from beauty and charm hadron decays, respectively, where the dashed lines indicate the FONLL uncertainties. (d) Measured ratio of electrons from beauty and charm hadron decays with error boxes depicting the total uncertainty.

cross sections have an additional normalization uncertainty of 3.5% [15].

In summary, invariant production cross sections of electrons from beauty and from charm hadron decays were measured in pp collisions at $\sqrt{s} = 7$ TeV. The agreement between theoretical predictions and the data suggests that FONLL pQCD calculations can reliably describe heavy-flavor production even at low p_T in the highest energy hadron collisions accessible in the laboratory today. Furthermore, these results provide a crucial baseline for heavy-flavor production studies in the hot and dense matter created in Pb-Pb collisions at the LHC.

The ALICE collaboration would like to thank all its engineers and technicians for their invaluable contributions to the construction of the experiment and the CERN accelerator teams for the outstanding performance of the LHC complex. The ALICE collaboration would like to thank M. Cacciari for provid-

ing the FONLL pQCD predictions for the cross sections of electrons from heavy-flavour hadron decays. The ALICE collaboration acknowledges the following funding agencies for their support in building and running the ALICE detector: State Committee of Science, Calouste Gulbenkian Foundation from Lisbon and Swiss Fonds Kidagan, Armenia; Conselho Nacional de Desenvolvimento Científico e Tecnológico (CNPq), Financiadora de Estudos e Projetos (FINEP), Fundação de Amparo à Pesquisa do Estado de São Paulo (FAPESP); National Natural Science Foundation of China (NSFC), the Chinese Ministry of Education (CMOE) and the Ministry of Science and Technology of China (MSTC); Ministry of Education and Youth of the Czech Republic; Danish Natural Science Research Council, the Carlsberg Foundation and the Danish National Research Foundation; The European Research Council under the European Community’s Seventh Framework Programme; Helsinki Institute of Physics and the Academy of Finland; French CNRS-IN2P3, the ‘Region Pays de Loire’, ‘Region Alsace’, ‘Region Auvergne’ and CEA, France; German BMBF and the Helmholtz Association; General Secretariat for Research and Technology, Ministry of Development, Greece; Hungarian OTKA and National Office for Research and Technology (NKTH); Department of Atomic Energy and Department of Science and Technology of the Government of India; Istituto Nazionale di Fisica Nucleare (INFN) and Centro Fermi - Museo Storico della Fisica e Centro Studi e Ricerche “Enrico Fermi”, Italy; MEXT Grant-in-Aid for Specially Promoted Research, Japan; Joint Institute for Nuclear Research, Dubna; National Research Foundation of Korea (NRF); CONACYT, DGAPA, México, ALFA-EC and the HELEN Program (High-Energy physics Latin-American–European Network); Stichting voor Fundamenteel Onderzoek der Materie (FOM) and the Nederlandse Organisatie voor Wetenschappelijk Onderzoek (NWO), Netherlands; Research Council of Norway (NFR); Polish Ministry of Science and Higher Education; National Authority for Scientific Research - NASR (Autoritatea Națională pentru Cercetare Științifică - ANCS); Ministry of Education and Science of Russian Federation, International Science and Technology Center, Russian Academy of Sciences, Russian Federal Agency of Atomic Energy, Russian Federal Agency for Science and Innovations and CERN-INTAS; Ministry of Education of Slovakia; Department of Science and Technology, South Africa; CIEMAT, EELA, Ministerio de Educación y Ciencia of Spain, Xunta de Galicia (Consellería de Educación), CEADEN, Cubaenergía, Cuba, and IAEA (International Atomic Energy Agency); Swedish Research Council (VR) and Knut & Alice Wallenberg Foundation (KAW); Ukraine Ministry of Education and Science; United Kingdom Science and Technology Facilities Council (STFC); The United States Department of Energy, the United States National Science Foundation, the State of Texas, and the State of Ohio.

References

- [1] D. Acosta et al. Measurement of the J/ψ meson and b -hadron production cross sections in $p\bar{p}$ collisions at $\sqrt{s} = 1960$ GeV. *Phys. Rev.*, D71:032001, 2005.
- [2] M. Cacciari, M. Greco, and P. Nason. The p_T spectrum in heavy-flavour hadroproduction. *JHEP*, 9805:007, 1998.
- [3] M. Cacciari, S. Frixione, and P. Nason. The p_T spectrum in heavy-flavour photoproduction. *JHEP*, 0103:006, 2001.
- [4] D. Acosta et al. Measurement of prompt charm meson production cross sections in $p\bar{p}$ collisions at $\sqrt{s} = 1.96$ TeV. *Phys. Rev. Lett.*, 91:241804, 2003.
- [5] A. Adare et al. Heavy-quark production in $p + p$ and energy loss and flow of heavy quarks in Au + Au collisions at $\sqrt{s_{NN}} = 200$ GeV. *Phys. Rev.*, C84:044905, 2011.
- [6] L. Adamczyk et al. Measurements of D^0 and D^* Production in $p + p$ Collisions at $\sqrt{s} = 200$ GeV. 2012. arXiv:1204.4244 [nucl-ex].
- [7] R. Aaij et al. Measurement of the B^\pm production cross-section in pp collisions at $\sqrt{s} = 7$ TeV. *JHEP*, 1204:093, 2012. and references therein.
- [8] S. Chatrchyan et al. Measurement of the B_s^0 production cross section with $B_s^0 \rightarrow J/\psi\phi$ decays in pp

- collisions at $\sqrt{s} = 7$ TeV. *Phys. Rev.*, D84:052008, 2011. and references therein.
- [9] B. Abelev et al. Measurement of prompt J/ψ and beauty hadron production cross sections at mid-rapidity in pp collisions at $\sqrt{s} = 7$ TeV. *Journal of High Energy Physics*, 2012:1–31, 2012.
- [10] K. Aamodt et al. Measurement of charm production at central rapidity in proton–proton collisions at $\sqrt{s} = 7$ TeV. *JHEP*, 01:128, 2012.
- [11] G. Aad et al. Measurements of the electron and muon inclusive cross-sections in pp collisions at $\sqrt{s} = 7$ TeV with the ATLAS detector. *Phys. Lett.*, B707:438–458, 2012.
- [12] B. Abelev et al. Measurement of electrons from semileptonic heavy-flavour hadron decays in pp collisions at $\sqrt{s} = 7$ TeV. *Phys. Rev.*, D86:112007, 2012. arXiv:1205.5423 [hep-ex].
- [13] B. Abelev et al. Heavy flavour decay muon production at forward rapidity in proton–proton collisions at $\sqrt{s} = 7$ TeV. *Phys. Lett.*, B708:265275, 2012.
- [14] K. Aamodt et al. The ALICE experiment at the CERN LHC. *JINST*, 3:S08002, 2008.
- [15] Betty Abelev et al. Measurement of inelastic, single- and double-diffraction cross sections in proton–proton collisions at the LHC with ALICE. 2012. arXiv:1208.4968 [hep-ex].
- [16] P. Billoir. Track fitting with multiple scattering: A new method. *Nucl. Instr. Meth.*, 225(2):352, 1984.
- [17] R. Brun et al., 1994. CERN Program Library Long Write-up, W5013.
- [18] T. Sjostrand, S. Mrenna, and P.Z. Skands. PYTHIA 6.4 Physics and Manual. *JHEP*, 0605:026, 2006.
- [19] P. Z. Skands. The Perugia Tunes. 2009.
- [20] Matteo Cacciari, Stefano Frixione, Nicolas Houdeau, Michelangelo L. Mangano, Paolo Nason, et al. Theoretical predictions for charm and bottom production at the LHC. *JHEP*, 1210:137, 2012.
- [21] B. Abelev et al. Neutral pion and η meson production in proton–proton collisions at $\sqrt{s} = 0.9$ TeV and $\sqrt{s} = 7$ TeV. *Phys.Lett.*, B717:162–172, 2012.
- [22] B. Abelev et al. D_s^+ meson production at central rapidity in proton–proton collisions at $\sqrt{s} = 7$ TeV. *Physics Letters B*, 718(2):279–294, 2012.
- [23] S. Chekanov et al. Measurement of charm fragmentation ratios and fractions in photoproduction at HERA. *Eur. Phys. J.*, C44:351–366, 2005.
- [24] S. Gorbunov and I. Kisel. Reconstruction of decay particles based on the Kalman filter, 2007. priv. commun.
- [25] J. Beringer et al. The Review of Particle Physics. *Phys. Rev.*, D86:010001, 2012.
- [26] P. M. Nadolsky et al. Implications of CTEQ global PDF analysis for collider observables. *Phys. Rev.*, D78:013004, 2008.
- [27] Louis Lyons, Duncan Gibaut, and Peter Clifford. How to combine correlated estimates of a single physical quantity. *Nucl.Instrum.Meth.*, A270:110, 1988.
- [28] Betty Abelev et al. Measurement of charm production at central rapidity in proton–proton collisions at $\sqrt{s} = 2.76$ TeV. *JHEP*, 1207:191, 2012.

A The ALICE Collaboration

B. Abelev⁶⁸, J. Adam³⁴, D. Adamová⁷³, A.M. Adare¹²⁰, M.M. Aggarwal⁷⁷, G. Aglieri Rinella³⁰, A.G. Agocs⁶⁰, A. Agostinelli¹⁹, S. Aguilar Salazar⁵⁶, Z. Ahammed¹¹⁶, N. Ahmad¹⁴, A. Ahmad Masoodi¹⁴, S.A. Ahn⁶², S.U. Ahn³⁷, A. Akindinov⁴⁶, D. Aleksandrov⁸⁸, B. Alessandro⁹⁴, R. Alfaro Molina⁵⁶, A. Alici^{97,10}, A. Alkin², E. Almaráz Aviña⁵⁶, J. Alme³², T. Alt³⁶, V. Altini²⁸, S. Altinpinar¹⁵, I. Altsybeev¹¹⁷, C. Andrei⁷⁰, A. Andronic⁸⁵, V. Anguelov⁸², J. Anielski⁵⁴, C. Anson¹⁶, T. Antičić⁸⁶, F. Antinori⁹³, P. Antonioli⁹⁷, L. Aphecetche¹⁰², H. Appelshäuser⁵², N. Arbor⁶⁴, S. Arcelli¹⁹, A. Arend⁵², N. Armesto¹³, R. Arnaldi⁹⁴, T. Aronsson¹²⁰, I.C. Arsene⁸⁵, M. Arslandok⁵², A. Asryan¹¹⁷, A. Augustinus³⁰, R. Averbeck⁸⁵, T.C. Awes⁷⁴, J. Äystö³⁸, M.D. Azmi^{14,79}, M. Bach³⁶, A. Badalá⁹⁹, Y.W. Baek^{63,37}, R. Bailhache⁵², R. Bala⁹⁴, R. Baldini Ferroli¹⁰, A. Baldisseri¹², A. Baldit⁶³, F. Baltasar Dos Santos Pedrosa³⁰, J. Bán⁴⁷, R.C. Baral⁴⁸, R. Barbera²⁵, F. Barile²⁸, G.G. Barnaföldi⁶⁰, L.S. Barnby⁹⁰, V. Barret⁶³, J. Bartke¹⁰⁴, M. Basile¹⁹, N. Bastid⁶³, S. Basu¹¹⁶, B. Bathen⁵⁴, G. Batigne¹⁰², B. Batyunya⁵⁹, C. Baumann⁵², I.G. Bearden⁷¹, H. Beck⁵², N.K. Behera⁴⁰, I. Belikov⁵⁸, F. Bellini¹⁹, R. Bellwied¹¹⁰, E. Belmont-Moreno⁵⁶, G. Bencedi⁶⁰, S. Beole²³, I. Berceanu⁷⁰, A. Bercuci⁷⁰, Y. Berdnikov⁷⁵, D. Berenyi⁶⁰, A.A.E. Bergognon¹⁰², D. Berzano⁹⁴, L. Betev³⁰, A. Bhasin⁸⁰, A.K. Bhati⁷⁷, J. Bhom¹¹⁴, L. Bianchi²³, N. Bianchi⁶⁵, C. Bianchin²⁰, J. Bielčik³⁴, J. Bielčiková⁷³, A. Bilandzic⁷¹, S. Bjelogrić⁴⁵, F. Blanco⁸, F. Blanco¹¹⁰, D. Blau⁸⁸, C. Blume⁵², M. Boccioli³⁰, N. Bock¹⁶, S. Böttger⁵¹, A. Bogdanov⁶⁹, H. Bøggild⁷¹, M. Bogolyubsky⁴³, L. Boldizsár⁶⁰, M. Bombara³⁵, J. Book⁵², H. Borel¹², A. Borissov¹¹⁹, S. Bose⁸⁹, F. Bossú^{79,23}, M. Botje⁷², E. Botta²³, B. Boyer⁴², E. Braidot⁶⁷, P. Braun-Munzinger⁸⁵, M. Bregant¹⁰², T. Breitner⁵¹, T.A. Browning⁸³, M. Broz³³, R. Brun³⁰, E. Bruna^{23,94}, G.E. Bruno²⁸, D. Budnikov⁸⁷, H. Buesching⁵², S. Bufalino^{23,94}, O. Busch⁸², Z. Buthelezi⁷⁹, D. Caballero Orduna¹²⁰, D. Caffarri^{20,93}, X. Cai⁵, H. Caines¹²⁰, E. Calvo Villar⁹¹, P. Camerini²¹, V. Canoa Roman⁹, G. Cara Romeo⁹⁷, F. Carena³⁰, W. Carena³⁰, N. Carlin Filho¹⁰⁷, F. Carminati³⁰, A. Casanova Díaz⁶⁵, J. Castillo Castellanos¹², J.F. Castillo Hernandez⁸⁵, E.A.R. Casula²², V. Catanescu⁷⁰, C. Cavicchioli³⁰, C. Ceballos Sanchez⁷, J. Cepila³⁴, P. Cerello⁹⁴, B. Chang^{38,123}, S. Chapeland³⁰, J.L. Charvet¹², S. Chattopadhyay¹¹⁶, S. Chattopadhyay⁸⁹, I. Chawla⁷⁷, M. Cherney⁷⁶, C. Cheshkov^{30,109}, B. Cheynis¹⁰⁹, V. Chibante Barroso³⁰, D.D. Chinellato¹⁰⁸, P. Chochula³⁰, M. Chojnacki⁴⁵, S. Choudhury¹¹⁶, P. Christakoglou⁷², C.H. Christensen⁷¹, P. Christiansen²⁹, T. Chujo¹¹⁴, S.U. Chung⁸⁴, C. Cicalo⁹⁶, L. Cifarelli^{19,30,10}, F. Cindolo⁹⁷, J. Cleymans⁷⁹, F. Coccetti¹⁰, F. Colamaria²⁸, D. Colella²⁸, G. Conesa Balbastre⁶⁴, Z. Conesa del Valle³⁰, P. Constantin⁸², G. Contin²¹, J.G. Contreras⁹, T.M. Cormier¹¹⁹, Y. Corrales Morales²³, P. Cortese²⁷, I. Cortés Maldonado¹, M.R. Cosentino⁶⁷, F. Costa³⁰, M.E. Cotallo⁸, E. Crescio⁹, P. Crochet⁶³, E. Cruz Alaniz⁵⁶, E. Cuautele⁵⁵, L. Cunqueiro⁶⁵, A. Dainese^{20,93}, H.H. Dalsgaard⁷¹, A. Danu⁵⁰, D. Das⁸⁹, I. Das⁴², K. Das⁸⁹, A. Dash¹⁰⁸, S. Dash⁴⁰, S. De¹¹⁶, G.O.V. de Barros¹⁰⁷, A. De Caro^{26,10}, G. de Cataldo⁹⁸, J. de Cuveland³⁶, A. De Falco²², D. De Gruttola²⁶, H. Delagrangé¹⁰², A. Deloff¹⁰⁰, V. Demanov⁸⁷, N. De Marco⁹⁴, E. Dénes⁶⁰, S. De Pasquale²⁶, A. Deppman¹⁰⁷, G. D'Erasmus²⁸, R. de Rooij⁴⁵, M.A. Diaz Corchero⁸, D. Di Bari²⁸, T. Dietel⁵⁴, C. Di Giglio²⁸, S. Di Liberto⁹⁵, A. Di Mauro³⁰, P. Di Nezza⁶⁵, R. Divià³⁰, Ø. Djuvsland¹⁵, A. Dobrin^{119,29}, T. Dobrowolski¹⁰⁰, I. Domínguez⁵⁵, B. Dönigus⁸⁵, O. Dordic¹⁸, O. Driga¹⁰², A.K. Dubey¹¹⁶, A. Dubla⁴⁵, L. Ducroux¹⁰⁹, P. Dupieux⁶³, M.R. Dutta Majumdar¹¹⁶, A.K. Dutta Majumdar⁸⁹, D. Elia⁹⁸, D. Emschermann⁵⁴, H. Engel⁵¹, B. Erazmus^{30,102}, H.A. Erdal³², B. Espagnon⁴², M. Estienne¹⁰², S. Esumi¹¹⁴, D. Evans⁹⁰, G. Eyyubova¹⁸, D. Fabris^{20,93}, J. Favre⁶⁴, D. Falchieri¹⁹, A. Fantoni⁶⁵, M. Fasel⁸⁵, R. Fearick⁷⁹, A. Fedunov⁵⁹, D. Fehler¹⁵, L. Feldkamp⁵⁴, D. Felea⁵⁰, B. Fenton-Olsen⁶⁷, G. Feofilov¹¹⁷, A. Fernández Téllez¹, A. Ferretti²³, R. Ferretti²⁷, A. Festanti²⁰, J. Figiel¹⁰⁴, M.A.S. Figueredo¹⁰⁷, S. Filchagin⁸⁷, D. Finogeev⁴⁴, F.M. Fionda²⁸, E.M. Fiore²⁸, M. Floris³⁰, S. Foertsch⁷⁹, P. Foka⁸⁵, S. Fokin⁸⁸, E. Fragiaco⁹², A. Francescon^{30,20}, U. Frankenfeld⁸⁵, U. Fuchs³⁰, C. Furget⁶⁴, M. Fusco Girard²⁶, J.J. Gaardhøje⁷¹, M. Gagliardi²³, A. Gago⁹¹, M. Gallio²³, D.R. Gangadharan¹⁶, P. Ganoti⁷⁴, C. Garabatos⁸⁵, E. Garcia-Solis¹¹, I. Garishvili⁶⁸, J. Gerhard³⁶, M. Germain¹⁰², C. Geuna¹², A. Gheata³⁰, M. Gheata^{50,30}, B. Ghidini²⁸, P. Ghosh¹¹⁶, P. Gianotti⁶⁵, M.R. Girard¹¹⁸, P. Giubellino³⁰, E. Gladysz-Dziadus¹⁰⁴, P. Glässel⁸², R. Gomez^{106,9}, E.G. Ferreira¹³, L.H. González-Trueba⁵⁶, P. González-Zamora⁸, S. Gorbunov³⁶, A. Goswami⁸¹, S. Gotovac¹⁰³, V. Grabski⁵⁶, L.K. Graczykowski¹¹⁸, R. Grajcarek⁸², A. Grelli⁴⁵, C. Grigoras³⁰, A. Grigoras³⁰, V. Grigoriev⁶⁹, A. Grigoryan¹²¹, S. Grigoryan⁵⁹, B. Grinyov², N. Grion⁹², P. Gros²⁹, J.F. Grosse-Oetringhaus³⁰, J.-Y. Grossiord¹⁰⁹, R. Grosso³⁰, F. Guber⁴⁴, R. Guernane⁶⁴, C. Guerra Gutierrez⁹¹, B. Guerzoni¹⁹, M. Guilbaud¹⁰⁹, K. Gulbrandsen⁷¹, T. Gunji¹¹³, A. Gupta⁸⁰, R. Gupta⁸⁰, H. Gutbrod⁸⁵, Ø. Haaland¹⁵, C. Hadjidakis⁴², M. Haiduc⁵⁰, H. Hamagaki¹¹³, G. Hamar⁶⁰, B.H. Han¹⁷, L.D. Hanratty⁹⁰, A. Hansen⁷¹, Z. Harmanová-Tóthová³⁵, J.W. Harris¹²⁰, M. Hartig⁵², D. Hasegan⁵⁰, D. Hatzifotiadou⁹⁷, A. Hayrapetyan^{30,121}, S.T. Heckel⁵², M. Heide⁵⁴, H. Helstrup³², A. Herghelegiu⁷⁰, G. Herrera Corral⁹, N. Herrmann⁸², B.A. Hess¹¹⁵, K.F. Hetland³², B. Hicks¹²⁰, P.T. Hille¹²⁰, B. Hippolyte⁵⁸, T. Horaguchi¹¹⁴, Y. Hori¹¹³, P. Hristov³⁰, I. Hřivnáčová⁴²,

M. Huang¹⁵, T.J. Humanic¹⁶, D.S. Hwang¹⁷, R. Ichou⁶³, R. Ilkaev⁸⁷, I. Ilkiv¹⁰⁰, M. Inaba¹¹⁴, E. Incani²², P.G. Innocenti³⁰, G.M. Innocenti²³, M. Ippolitov⁸⁸, M. Irfan¹⁴, C. Ivan⁸⁵, V. Ivanov⁷⁵, A. Ivanov¹¹⁷, M. Ivanov⁸⁵, O. Ivanytskyi², P. M. Jacobs⁶⁷, H.J. Jang⁶², M.A. Janik¹¹⁸, R. Janik³³, P.H.S.Y. Jayarathna¹¹⁰, S. Jena⁴⁰, D.M. Jha¹¹⁹, R.T. Jimenez Bustamante⁵⁵, L. Jirde³⁰, P.G. Jones⁹⁰, H. Jung³⁷, A. Jusko⁹⁰, A.B. Kaidalov⁴⁶, V. Kakoyan¹²¹, S. Kalcher³⁶, P. Kaliňák⁴⁷, T. Kalliokoski³⁸, A. Kalweit^{53,30}, J.H. Kang¹²³, V. Kaplin⁶⁹, A. Karasu Uysal^{30,122}, O. Karavichev⁴⁴, T. Karavicheva⁴⁴, E. Karpechev⁴⁴, A. Kazantsev⁸⁸, U. Kebschull⁵¹, R. Keidel¹²⁴, M.M. Khan¹⁴, S.A. Khan¹¹⁶, P. Khan⁸⁹, A. Khanzadeev⁷⁵, Y. Kharlov⁴³, B. Kileng³², M. Kim¹²³, D.W. Kim³⁷, J.H. Kim¹⁷, J.S. Kim³⁷, M. Kim³⁷, S. Kim¹⁷, D.J. Kim³⁸, B. Kim¹²³, T. Kim¹²³, S. Kirsch³⁶, I. Kisel³⁶, S. Kiselev⁴⁶, A. Kisiel¹¹⁸, J.L. Klay⁴, J. Klein⁸², C. Klein-Bösing⁵⁴, M. Kliemant⁵², A. Kluge³⁰, M.L. Knichel⁸⁵, A.G. Knospe¹⁰⁵, K. Koch⁸², M.K. Köhler⁸⁵, T. Kollegger³⁶, A. Kolojvari¹¹⁷, V. Kondratiev¹¹⁷, N. Kondratyeva⁶⁹, A. Konevskikh⁴⁴, A. Korneev⁸⁷, R. Kour⁹⁰, M. Kowalski¹⁰⁴, S. Kox⁶⁴, G. Koyithatta Meethalevedu⁴⁰, J. Kral³⁸, I. Králik⁴⁷, F. Kramer⁵², I. Kraus⁸⁵, T. Krawutschke^{82,31}, M. Krelina³⁴, M. Kretz³⁶, M. Krivda^{90,47}, F. Krizek³⁸, M. Krus³⁴, E. Kryshen⁷⁵, M. Krzewicki⁸⁵, Y. Kucheriaev⁸⁸, T. Kugathasan³⁰, C. Kuhn⁵⁸, P.G. Kuijter⁷², I. Kulakov⁵², J. Kumar⁴⁰, P. Kurashvili¹⁰⁰, A. Kurepin⁴⁴, A.B. Kurepin⁴⁴, A. Kuryakin⁸⁷, S. Kuschpil⁷³, V. Kuschpil⁷³, H. Kvaerno¹⁸, M.J. Kwon⁸², Y. Kwon¹²³, P. Ladrón de Guevara⁵⁵, I. Lakomov⁴², R. Langoy¹⁵, S.L. La Pointe⁴⁵, C. Lara⁵¹, A. Lardeux¹⁰², P. La Rocca²⁵, R. Lea²¹, Y. Le Bornec⁴², M. Lechman³⁰, K.S. Lee³⁷, S.C. Lee³⁷, G.R. Lee⁹⁰, F. Lefèvre¹⁰², J. Lehnert⁵², M. Lenhardt⁸⁵, V. Lenti⁹⁸, H. León⁵⁶, M. Leoncino⁹⁴, I. León Monzón¹⁰⁶, H. León Vargas⁵², P. Lévai⁶⁰, J. Lien¹⁵, R. Lietava⁹⁰, S. Lindal¹⁸, V. Lindenstruth³⁶, C. Lippmann^{85,30}, M.A. Lisa¹⁶, L. Liu¹⁵, V.R. Loggins¹¹⁹, V. Loginov⁶⁹, S. Lohn³⁰, D. Lohner⁸², C. Loizides⁶⁷, K.K. Loo³⁸, X. Lopez⁶³, E. López Torres⁷, G. Løvnhøiden¹⁸, X.-G. Lu⁸², P. Luetig⁵², M. Lunardon²⁰, J. Luo⁵, G. Luparello⁴⁵, L. Luquin¹⁰², C. Luzzi³⁰, R. Ma¹²⁰, K. Ma⁵, D.M. Madagodahettige-Don¹¹⁰, A. Maevskaya⁴⁴, M. Mager^{53,30}, D.P. Mahapatra⁴⁸, A. Maire⁸², M. Malaev⁷⁵, I. Maldonado Cervantes⁵⁵, L. Malinina^{59,ii}, D. Mal'Kevich⁴⁶, P. Malzacher⁸⁵, A. Mamonov⁸⁷, L. Mangotra⁸⁰, V. Manko⁸⁸, F. Manso⁶³, V. Manzari⁹⁸, Y. Mao⁵, M. Marchisone^{63,23}, J. Mareš⁴⁹, G.V. Margagliotti^{21,92}, A. Margotti⁹⁷, A. Marín⁸⁵, C.A. Marin Tobon³⁰, C. Markert¹⁰⁵, I. Martashvili¹¹², P. Martinengo³⁰, M.I. Martínez¹, A. Martínez Davalos⁵⁶, G. Martínez García¹⁰², Y. Martynov², A. Mas¹⁰², S. Masciocchi⁸⁵, M. Masera²³, A. Masoni⁹⁶, L. Massacrier¹⁰², A. Mastroserio²⁸, Z.L. Matthews⁹⁰, A. Matyjka^{104,102}, C. Mayer¹⁰⁴, J. Mazer¹¹², M.A. Mazzoni⁹⁵, F. Meddi²⁴, A. Menchaca-Rocha⁵⁶, J. Mercado Pérez⁸², M. Meres³³, Y. Miake¹¹⁴, L. Milano²³, J. Milosevic^{18,ii}, A. Mischke⁴⁵, A.N. Mishra⁸¹, D. Miśkowiec^{85,30}, C. Mitu⁵⁰, J. Mlynar¹¹⁹, B. Mohanty¹¹⁶, L. Molnar^{60,30}, L. Montaño Zetina⁹, M. Monteno⁹⁴, E. Montes⁸, T. Moon¹²³, M. Morando²⁰, D.A. Moreira De Godoy¹⁰⁷, S. Moretto²⁰, A. Morsch³⁰, V. Muccifora⁶⁵, E. Mudnic¹⁰³, S. Muhuri¹¹⁶, M. Mukherjee¹¹⁶, H. Müller³⁰, M.G. Munhoz¹⁰⁷, L. Musa³⁰, A. Musso⁹⁴, B.K. Nandi⁴⁰, R. Nania⁹⁷, E. Nappi⁹⁸, C. Nattrass¹¹², N.P. Naumov⁸⁷, S. Navin⁹⁰, T.K. Nayak¹¹⁶, S. Nazarenko⁸⁷, G. Nazarov⁸⁷, A. Nedosekin⁴⁶, M. Nicassio²⁸, M. Niclescu^{50,30}, B.S. Nielsen⁷¹, T. Niida¹¹⁴, S. Nikolaev⁸⁸, V. Nikolic⁸⁶, S. Nikulin⁸⁸, V. Nikulin⁷⁵, B.S. Nilsen⁷⁶, M.S. Nilsson¹⁸, F. Noferini^{97,10}, P. Nomokonov⁵⁹, G. Nooren⁴⁵, N. Novitzky³⁸, A. Nyman⁸⁸, A. Nyatha⁴⁰, C. Nygaard⁷¹, J. Nystrand¹⁵, A. Ochirov¹¹⁷, H. Oeschler^{53,30}, S. Oh¹²⁰, S.K. Oh³⁷, J. Oleniacz¹¹⁸, C. Oppedisano⁹⁴, A. Ortiz Velasquez^{29,55}, G. Ortona²³, A. Oskarsson²⁹, P. Ostrowski¹¹⁸, J. Otwinowski⁸⁵, K. Oyama⁸², K. Ozawa¹¹³, Y. Pachmayer⁸², M. Pachr³⁴, F. Padilla²³, P. Pagano²⁶, G. Paic⁵⁵, F. Painke³⁶, C. Pajares¹³, S.K. Pal¹¹⁶, A. Palaha⁹⁰, A. Palmeri⁹⁹, V. Papikyan¹²¹, G.S. Pappalardo⁹⁹, W.J. Park⁸⁵, A. Passfeld⁵⁴, B. Pastirčák⁴⁷, D.I. Patalakha⁴³, V. Paticchio⁹⁸, A. Pavlinov¹¹⁹, T. Pawlak¹¹⁸, T. Peitzmann⁴⁵, H. Pereira Da Costa¹², E. Pereira De Oliveira Filho¹⁰⁷, D. Peresunko⁸⁸, C.E. Pérez Lara⁷², E. Perez Lezama⁵⁵, D. Perini³⁰, D. Perrino²⁸, W. Peryt¹¹⁸, A. Pesci⁹⁷, V. Peskov^{30,55}, Y. Pestov³, V. Petráček³⁴, M. Petran³⁴, M. Petris⁷⁰, P. Petrov⁹⁰, M. Petrovici⁷⁰, C. Petta²⁵, S. Piano⁹², A. Piccotti⁹⁴, M. Pikna³³, P. Pillot¹⁰², O. Pinazza³⁰, L. Pinsky¹¹⁰, N. Pitz⁵², D.B. Piyarathna¹¹⁰, M. Planinic⁸⁶, M. Płoskoń⁶⁷, J. Pluta¹¹⁸, T. Pochepstov⁵⁹, S. Pochybova⁶⁰, P.L.M. Podesta-Lerma¹⁰⁶, M.G. Poghosyan^{30,23}, K. Polák⁴⁹, B. Polichtchouk⁴³, A. Pop⁷⁰, S. Porteboeuf-Houssais⁶³, V. Pospíšil³⁴, B. Potukuchi⁸⁰, S.K. Prasad¹¹⁹, R. Preghenella^{97,10}, F. Prino⁹⁴, C.A. Pruneau¹¹⁹, I. Pshenichnov⁴⁴, S. Puchagin⁸⁷, G. Puudu²², A. Pulvirenti²⁵, V. Punin⁸⁷, M. Putis³⁵, J. Putschke^{119,120}, E. Quercigh³⁰, H. Qvigstad¹⁸, A. Rachevski⁹², A. Rademakers³⁰, T.S. Rähä³⁸, J. Rak³⁸, A. Rakotozafindrabe¹², L. Ramello²⁷, A. Ramírez Reyes⁹, R. Raniwala⁸¹, S. Raniwala⁸¹, S.S. Räsänen³⁸, B.T. Rascanu⁵², D. Rathee⁷⁷, K.F. Read¹¹², J.S. Real⁶⁴, K. Redlich^{100,57}, P. Reichelt⁵², M. Reicher⁴⁵, R. Renfordt⁵², A.R. Reolon⁶⁵, A. Reshetin⁴⁴, F. Rettig³⁶, J.-P. Revol³⁰, K. Reygers⁸², L. Riccati⁹⁴, R.A. Ricci⁶⁶, T. Richert²⁹, M. Richter¹⁸, P. Riedler³⁰, W. Riegler³⁰, F. Riggi^{25,99}, B. Rodrigues Fernandes Rabacal³⁰, M. Rodríguez Cahuantzi¹, A. Rodríguez Manso⁷², K. Røed¹⁵, D. Rohr³⁶, D. Röhrich¹⁵, R. Romita⁸⁵, F. Ronchetti⁶⁵, P. Rosnet⁶³, S. Rossegger³⁰, A. Rossi^{30,20}, C. Roy⁵⁸, P. Roy⁸⁹, A.J. Rubio Montero⁸, R. Rui²¹,

R. Russo²³, E. Ryabinkin⁸⁸, A. Rybicki¹⁰⁴, S. Sadovsky⁴³, K. Šafařík³⁰, R. Sahoo⁴¹, P.K. Sahu⁴⁸, J. Saini¹¹⁶, H. Sakaguchi³⁹, S. Sakai⁶⁷, D. Sakata¹¹⁴, C.A. Salgado¹³, J. Salzwedel¹⁶, S. Sambyal⁸⁰, V. Samsonov⁷⁵, X. Sanchez Castro⁵⁸, L. Šándor⁴⁷, A. Sandoval⁵⁶, S. Sano¹¹³, M. Sano¹¹⁴, R. Santo⁵⁴, R. Santoro^{98,30,10}, J. Sarkamo³⁸, E. Scapparone⁹⁷, F. Scarlassara²⁰, R.P. Scharenberg⁸³, C. Schiaua⁷⁰, R. Schicker⁸², C. Schmidt⁸⁵, H.R. Schmidt¹¹⁵, S. Schreiner³⁰, S. Schuchmann⁵², J. Schukraft³⁰, Y. Schutz^{30,102}, K. Schwarz⁸⁵, K. Schweda^{85,82}, G. Scioli¹⁹, E. Scomparin⁹⁴, R. Scott¹¹², G. Segato²⁰, I. Selyuzhenkov⁸⁵, S. Senyukov⁵⁸, J. Seo⁸⁴, S. Serchi²², E. Serradilla^{8,56}, A. Sevcenco⁵⁰, A. Shabetai¹⁰², G. Shabratova⁵⁹, R. Shahoyan³⁰, S. Sharma⁸⁰, N. Sharma⁷⁷, S. Rohni⁸⁰, K. Shigaki³⁹, M. Shimomura¹¹⁴, K. Shtejer⁷, Y. Sibiriak⁸⁸, M. Siciliano²³, E. Sicking³⁰, S. Siddhanta⁹⁶, T. Siemiarczuk¹⁰⁰, D. Silvermyr⁷⁴, C. Silvestre⁶⁴, G. Simatovic^{55,86}, G. Simonetti³⁰, R. Singaraju¹¹⁶, R. Singh⁸⁰, S. Singha¹¹⁶, V. Singhal¹¹⁶, B.C. Sinha¹¹⁶, T. Sinha⁸⁹, B. Sitar³³, M. Sitta²⁷, T.B. Skaali¹⁸, K. Skjerdal¹⁵, R. Smakal³⁴, N. Smirnov¹²⁰, R.J.M. Snellings⁴⁵, C. Sjøgaard⁷¹, R. Soltz⁶⁸, H. Son¹⁷, J. Song⁸⁴, M. Song¹²³, C. Soos³⁰, F. Soramel²⁰, I. Sputowska¹⁰⁴, M. Spyropoulou-Stassinaki⁷⁸, B.K. Srivastava⁸³, J. Stachel⁸², I. Stan⁵⁰, I. Stan⁵⁰, G. Stefanek¹⁰⁰, M. Steinpreis¹⁶, E. Stenlund²⁹, G. Steyn⁷⁹, J.H. Stiller⁸², D. Stocco¹⁰², M. Stolpovskiy⁴³, K. Strabykin⁸⁷, P. Strmen³³, A.A.P. Suaide¹⁰⁷, M.A. Subieta Vásquez²³, T. Sugitate³⁹, C. Suire⁴², M. Sukhorukov⁸⁷, R. Sultanov⁴⁶, M. Šumbera⁷³, T. Susa⁸⁶, T.J.M. Symons⁶⁷, A. Szanto de Toledo¹⁰⁷, I. Szarka³³, A. Szczepankiewicz^{104,30}, A. Szostak¹⁵, M. Szymański¹¹⁸, J. Takahashi¹⁰⁸, J.D. Tapia Takaki⁴², A. Tauro³⁰, G. Tejada Muñoz¹, A. Telesca³⁰, C. Terrevoli²⁸, J. Thäder⁸⁵, D. Thomas⁴⁵, R. Tieulent¹⁰⁹, A.R. Timmins¹¹⁰, D. Tlusty³⁴, A. Toia^{36,20,93}, H. Torii¹¹³, L. Toscano⁹⁴, V. Trubnikov², D. Truesdale¹⁶, W.H. Trzaska³⁸, T. Tsuji¹¹³, A. Tumkin⁸⁷, R. Turrisi⁹³, T.S. Tveter¹⁸, J. Ulery⁵², K. Ullaland¹⁵, J. Ulrich^{61,51}, A. Uras¹⁰⁹, J. Urbán³⁵, G.M. Urciuoli⁹⁵, G.L. Usai²², M. Vajzer^{34,73}, M. Vala^{59,47}, L. Valencia Palomo⁴², S. Vallero⁸², P. Vande Vyvre³⁰, M. van Leeuwen⁴⁵, L. Vannucci⁶⁶, A. Vargas¹, R. Varma⁴⁰, M. Vasileiou⁷⁸, A. Vasiliev⁸⁸, V. Vechernin¹¹⁷, M. Veldhoen⁴⁵, M. Venaruzzo²¹, E. Vercellin²³, S. Vergara¹, R. Vernet⁶, M. Verweij⁴⁵, L. Vickovic¹⁰³, G. Viesti²⁰, O. Vikhlyantsev⁸⁷, Z. Vilakazi⁷⁹, O. Villalobos Baillie⁹⁰, Y. Vinogradov⁸⁷, L. Vinogradov¹¹⁷, A. Vinogradov⁸⁸, T. Virgili²⁶, Y.P. Viyogi¹¹⁶, A. Vodopyanov⁵⁹, K. Voloshin⁴⁶, S. Voloshin¹¹⁹, G. Volpe^{28,30}, B. von Haller³⁰, D. Vranic⁸⁵, G. Øvrebek¹⁵, J. Vrláková³⁵, B. Vulpescu⁶³, A. Vyushin⁸⁷, V. Wagner³⁴, B. Wagner¹⁵, R. Wan⁵, D. Wang⁵, M. Wang⁵, Y. Wang⁵, Y. Wang⁸², K. Watanabe¹¹⁴, M. Weber¹¹⁰, J.P. Wessels^{30,54}, U. Westerhoff⁵⁴, J. Wiechula¹¹⁵, J. Wikne¹⁸, M. Wilde⁵⁴, A. Wilk⁵⁴, G. Wilk¹⁰⁰, M.C.S. Williams⁹⁷, B. Windelband⁸², L. Xaplanteris Karampatsos¹⁰⁵, C.G. Yaldo¹¹⁹, Y. Yamaguchi¹¹³, S. Yang¹⁵, H. Yang¹², S. Yasnopolskiy⁸⁸, J. Yi⁸⁴, Z. Yin⁵, I.-K. Yoo⁸⁴, J. Yoon¹²³, W. Yu⁵², X. Yuan⁵, I. Yushmanov⁸⁸, V. Zaccaro⁷¹, C. Zach³⁴, C. Zampolli⁹⁷, S. Zaporozhets⁵⁹, A. Zarochentsev¹¹⁷, P. Závada⁴⁹, N. Zaviyalov⁸⁷, H. Zbroszczyk¹¹⁸, P. Zelnicek⁵¹, I.S. Zgura⁵⁰, M. Zhalov⁷⁵, X. Zhang^{63,5}, H. Zhang⁵, F. Zhou⁵, Y. Zhou⁴⁵, D. Zhou⁵, J. Zhu⁵, X. Zhu⁵, J. Zhu⁵, A. Zichichi^{19,10}, A. Zimmermann⁸², G. Zinovjev², Y. Zoccarato¹⁰⁹, M. Zynovyev², M. Zyzak⁵²

Affiliation notes

- ⁱ Also at: M.V.Lomonosov Moscow State University, D.V.Skobeltzyn Institute of Nuclear Physics, Moscow, Russia
- ⁱⁱ Also at: University of Belgrade, Faculty of Physics and "Vinča" Institute of Nuclear Sciences, Belgrade, Serbia

Collaboration Institutes

- ¹ Benemérita Universidad Autónoma de Puebla, Puebla, Mexico
- ² Bogolyubov Institute for Theoretical Physics, Kiev, Ukraine
- ³ Budker Institute for Nuclear Physics, Novosibirsk, Russia
- ⁴ California Polytechnic State University, San Luis Obispo, California, United States
- ⁵ Central China Normal University, Wuhan, China
- ⁶ Centre de Calcul de l'IN2P3, Villeurbanne, France
- ⁷ Centro de Aplicaciones Tecnológicas y Desarrollo Nuclear (CEADEN), Havana, Cuba
- ⁸ Centro de Investigaciones Energéticas Medioambientales y Tecnológicas (CIEMAT), Madrid, Spain
- ⁹ Centro de Investigación y de Estudios Avanzados (CINVESTAV), Mexico City and Mérida, Mexico
- ¹⁰ Centro Fermi – Centro Studi e Ricerche e Museo Storico della Fisica "Enrico Fermi", Rome, Italy
- ¹¹ Chicago State University, Chicago, United States
- ¹² Commissariat à l'Energie Atomique, IRFU, Saclay, France

- 13 Departamento de Física de Partículas and IGFAE, Universidad de Santiago de Compostela, Santiago de Compostela, Spain
- 14 Department of Physics Aligarh Muslim University, Aligarh, India
- 15 Department of Physics and Technology, University of Bergen, Bergen, Norway
- 16 Department of Physics, Ohio State University, Columbus, Ohio, United States
- 17 Department of Physics, Sejong University, Seoul, South Korea
- 18 Department of Physics, University of Oslo, Oslo, Norway
- 19 Dipartimento di Fisica dell'Università and Sezione INFN, Bologna, Italy
- 20 Dipartimento di Fisica dell'Università and Sezione INFN, Padova, Italy
- 21 Dipartimento di Fisica dell'Università and Sezione INFN, Trieste, Italy
- 22 Dipartimento di Fisica dell'Università and Sezione INFN, Cagliari, Italy
- 23 Dipartimento di Fisica dell'Università and Sezione INFN, Turin, Italy
- 24 Dipartimento di Fisica dell'Università 'La Sapienza' and Sezione INFN, Rome, Italy
- 25 Dipartimento di Fisica e Astronomia dell'Università and Sezione INFN, Catania, Italy
- 26 Dipartimento di Fisica 'E.R. Caianiello' dell'Università and Gruppo Collegato INFN, Salerno, Italy
- 27 Dipartimento di Scienze e Innovazione Tecnologica dell'Università del Piemonte Orientale and Gruppo Collegato INFN, Alessandria, Italy
- 28 Dipartimento Interateneo di Fisica 'M. Merlin' and Sezione INFN, Bari, Italy
- 29 Division of Experimental High Energy Physics, University of Lund, Lund, Sweden
- 30 European Organization for Nuclear Research (CERN), Geneva, Switzerland
- 31 Fachhochschule Köln, Köln, Germany
- 32 Faculty of Engineering, Bergen University College, Bergen, Norway
- 33 Faculty of Mathematics, Physics and Informatics, Comenius University, Bratislava, Slovakia
- 34 Faculty of Nuclear Sciences and Physical Engineering, Czech Technical University in Prague, Prague, Czech Republic
- 35 Faculty of Science, P.J. Šafárik University, Košice, Slovakia
- 36 Frankfurt Institute for Advanced Studies, Johann Wolfgang Goethe-Universität Frankfurt, Frankfurt, Germany
- 37 Gangneung-Wonju National University, Gangneung, South Korea
- 38 Helsinki Institute of Physics (HIP) and University of Jyväskylä, Jyväskylä, Finland
- 39 Hiroshima University, Hiroshima, Japan
- 40 Indian Institute of Technology Bombay (IIT), Mumbai, India
- 41 Indian Institute of Technology Indore (IIT), Indore, India
- 42 Institut de Physique Nucléaire d'Orsay (IPNO), Université Paris-Sud, CNRS-IN2P3, Orsay, France
- 43 Institute for High Energy Physics, Protvino, Russia
- 44 Institute for Nuclear Research, Academy of Sciences, Moscow, Russia
- 45 Nikhef, National Institute for Subatomic Physics and Institute for Subatomic Physics of Utrecht University, Utrecht, Netherlands
- 46 Institute for Theoretical and Experimental Physics, Moscow, Russia
- 47 Institute of Experimental Physics, Slovak Academy of Sciences, Košice, Slovakia
- 48 Institute of Physics, Bhubaneswar, India
- 49 Institute of Physics, Academy of Sciences of the Czech Republic, Prague, Czech Republic
- 50 Institute of Space Sciences (ISS), Bucharest, Romania
- 51 Institut für Informatik, Johann Wolfgang Goethe-Universität Frankfurt, Frankfurt, Germany
- 52 Institut für Kernphysik, Johann Wolfgang Goethe-Universität Frankfurt, Frankfurt, Germany
- 53 Institut für Kernphysik, Technische Universität Darmstadt, Darmstadt, Germany
- 54 Institut für Kernphysik, Westfälische Wilhelms-Universität Münster, Münster, Germany
- 55 Instituto de Ciencias Nucleares, Universidad Nacional Autónoma de México, Mexico City, Mexico
- 56 Instituto de Física, Universidad Nacional Autónoma de México, Mexico City, Mexico
- 57 Institut of Theoretical Physics, University of Wrocław
- 58 Institut Pluridisciplinaire Hubert Curien (IPHC), Université de Strasbourg, CNRS-IN2P3, Strasbourg, France
- 59 Joint Institute for Nuclear Research (JINR), Dubna, Russia
- 60 KFKI Research Institute for Particle and Nuclear Physics, Hungarian Academy of Sciences, Budapest, Hungary
- 61 Kirchhoff-Institut für Physik, Ruprecht-Karls-Universität Heidelberg, Heidelberg, Germany

- 62 Korea Institute of Science and Technology Information, Daejeon, South Korea
- 63 Laboratoire de Physique Corpusculaire (LPC), Clermont Université, Université Blaise Pascal, CNRS-IN2P3, Clermont-Ferrand, France
- 64 Laboratoire de Physique Subatomique et de Cosmologie (LPSC), Université Joseph Fourier, CNRS-IN2P3, Institut Polytechnique de Grenoble, Grenoble, France
- 65 Laboratori Nazionali di Frascati, INFN, Frascati, Italy
- 66 Laboratori Nazionali di Legnaro, INFN, Legnaro, Italy
- 67 Lawrence Berkeley National Laboratory, Berkeley, California, United States
- 68 Lawrence Livermore National Laboratory, Livermore, California, United States
- 69 Moscow Engineering Physics Institute, Moscow, Russia
- 70 National Institute for Physics and Nuclear Engineering, Bucharest, Romania
- 71 Niels Bohr Institute, University of Copenhagen, Copenhagen, Denmark
- 72 Nikhef, National Institute for Subatomic Physics, Amsterdam, Netherlands
- 73 Nuclear Physics Institute, Academy of Sciences of the Czech Republic, Řež u Prahy, Czech Republic
- 74 Oak Ridge National Laboratory, Oak Ridge, Tennessee, United States
- 75 Petersburg Nuclear Physics Institute, Gatchina, Russia
- 76 Physics Department, Creighton University, Omaha, Nebraska, United States
- 77 Physics Department, Panjab University, Chandigarh, India
- 78 Physics Department, University of Athens, Athens, Greece
- 79 Physics Department, University of Cape Town, iThemba LABS, Cape Town, South Africa
- 80 Physics Department, University of Jammu, Jammu, India
- 81 Physics Department, University of Rajasthan, Jaipur, India
- 82 Physikalisches Institut, Ruprecht-Karls-Universität Heidelberg, Heidelberg, Germany
- 83 Purdue University, West Lafayette, Indiana, United States
- 84 Pusan National University, Pusan, South Korea
- 85 Research Division and ExtreMe Matter Institute EMMI, GSI Helmholtzzentrum für Schwerionenforschung, Darmstadt, Germany
- 86 Rudjer Bošković Institute, Zagreb, Croatia
- 87 Russian Federal Nuclear Center (VNIIEF), Sarov, Russia
- 88 Russian Research Centre Kurchatov Institute, Moscow, Russia
- 89 Saha Institute of Nuclear Physics, Kolkata, India
- 90 School of Physics and Astronomy, University of Birmingham, Birmingham, United Kingdom
- 91 Sección Física, Departamento de Ciencias, Pontificia Universidad Católica del Perú, Lima, Peru
- 92 Sezione INFN, Trieste, Italy
- 93 Sezione INFN, Padova, Italy
- 94 Sezione INFN, Turin, Italy
- 95 Sezione INFN, Rome, Italy
- 96 Sezione INFN, Cagliari, Italy
- 97 Sezione INFN, Bologna, Italy
- 98 Sezione INFN, Bari, Italy
- 99 Sezione INFN, Catania, Italy
- 100 Soltan Institute for Nuclear Studies, Warsaw, Poland
- 101 Nuclear Physics Group, STFC Daresbury Laboratory, Daresbury, United Kingdom
- 102 SUBATECH, Ecole des Mines de Nantes, Université de Nantes, CNRS-IN2P3, Nantes, France
- 103 Technical University of Split FESB, Split, Croatia
- 104 The Henryk Niewodniczanski Institute of Nuclear Physics, Polish Academy of Sciences, Cracow, Poland
- 105 The University of Texas at Austin, Physics Department, Austin, TX, United States
- 106 Universidad Autónoma de Sinaloa, Culiacán, Mexico
- 107 Universidade de São Paulo (USP), São Paulo, Brazil
- 108 Universidade Estadual de Campinas (UNICAMP), Campinas, Brazil
- 109 Université de Lyon, Université Lyon 1, CNRS-IN2P3, IPN-Lyon, Villeurbanne, France
- 110 University of Houston, Houston, Texas, United States
- 111 University of Technology and Austrian Academy of Sciences, Vienna, Austria
- 112 University of Tennessee, Knoxville, Tennessee, United States
- 113 University of Tokyo, Tokyo, Japan
- 114 University of Tsukuba, Tsukuba, Japan

- ¹¹⁵ Eberhard Karls Universität Tübingen, Tübingen, Germany
- ¹¹⁶ Variable Energy Cyclotron Centre, Kolkata, India
- ¹¹⁷ V. Fock Institute for Physics, St. Petersburg State University, St. Petersburg, Russia
- ¹¹⁸ Warsaw University of Technology, Warsaw, Poland
- ¹¹⁹ Wayne State University, Detroit, Michigan, United States
- ¹²⁰ Yale University, New Haven, Connecticut, United States
- ¹²¹ Yerevan Physics Institute, Yerevan, Armenia
- ¹²² Yildiz Technical University, Istanbul, Turkey
- ¹²³ Yonsei University, Seoul, South Korea
- ¹²⁴ Zentrum für Technologietransfer und Telekommunikation (ZTT), Fachhochschule Worms, Worms, Germany